

Graphene Oxide as a Novel Nanoplatforam for Electrochemical Detection of Arsenic (III)

Maria Sarno^{a,b}, Carmela Scudieri^{a*}, Andrea Longo^a, Paolo Ciambelli^{a,b}

^a Department of Industrial Engineering, University of Salerno, via Giovanni Paolo II, 132 - 84084 Fisciano (SA), Italy

^b NANO_MATES Research Centre, University of Salerno, via Giovanni Paolo II, 132 - 84084 Fisciano (SA), Italy
cscudieri@unisa.it

In this paper, we present a novel and stable electrochemical sensor made of a magnetite/graphene oxide (Fe₃O₄/rGO) nanocomposite. It was deposited on a glassy carbon electrode for electroanalytical detection of As³⁺, via cyclic voltammetry and square wave anodic stripping voltammetry in phosphate buffer solutions. The electrode shows a very good relation between current response and amount of arsenic in a concentration of pollutants ranging from micromolar to nanomolar. Our sensor is easy to use, inexpensive and has allowed sensitive detection of As in non-acidic media (pH=7).

1. Introduction

Arsenic exists in many different chemical forms in nature, particularly, in groundwater they are found almost exclusively as arsenite (AsO₂⁻, As³⁺) and arsenate (HAsO₄²⁻, As⁵⁺). Arsenic compounds are known to be toxic and the exposure of humans, animals and ecosystems remains an international concern (Majid et al., 2006). Furthermore, the toxicity of arsenic is greatly dependent on As³⁺ that is 50 times more toxic than arsenate (Mandal et al., 2002). The maximum permissible arsenic contaminant level for the World Health Organization's (WHO) in drinking water is 10 µg L⁻¹ (World Health Organization, 2004). Therefore, arsenic poisoning is an urgent problem requiring easy and efficient detection strategies. To date, a variety of analytical methods have been applied to detect arsenic including inductively coupled plasma mass spectrometry (ICP) (Alvarez-Llamas et al., 2005) atomic fluorescence spectrometry (Cai et al., 2000), and graphite furnace atomic adsorption spectrometry (Zhang et al., 2011). These methods require the use of expensive instrumentation and high operating costs for arsenic detection (Story et al., 1992). However, electrochemical methods are the most promising techniques, because they are cheap and can provide very accurate measurements with a rapid analysis time (Vandehecke et al., 2007). As reported in the recent studies, electrochemical detection of As³⁺, has been achieved using the hanging mercury drop electrode (Vandehecke et al., 2007) and the mercury film electrode (Sun et al., 1997). Moreover, due to the potential toxicity of mercury together with operational limitations, portable sensors utilizing mercury electrodes were subsequently replaced by other solid metal substrates, such as platinum (Hignett et al., 2004), gold (Simm et al., 2004), and silver (Ivandini et al., 2007). Among these, gold was found to be the superior substrate for the working electrode (Sun et al., 1997). However, gold is not cost-effective for commercial products. Furthermore, the gold-based electrodes need to be operated in strongly acid media which could cause the problems of producing toxic arsine gas, generating interface from H₂ evolution and causing unsafety for transport. In addition, surface fouling is a common problem which needs to be resolved (Ivandini et al., 2007).

On the other hand, from these results emerged that some problems can be associated with arsenic voltammetry at solid electrodes, such as: limited sensitivity, low electron transfer kinetics, high overpotential at which electron transfer process occurs, low stability over a wide range of solution composition, and no reproducibility of the electrode surfaces between each measurements. In an effort to overcome these limitations, it was found the higher sensitivity of the anodic stripping potentiometric or voltammetric detection of arsenic (Sun et al., 1997). On the other hand, nanometer size materials (Welch et al., 2006; Yang et al., 2006), have been used successfully for electroanalytical detection of As³⁺ using cyclic voltammetry (CV) or anodic stripping voltammetry techniques. In particular, glassy carbon electrode (GCE) modified with

nanoparticles (NPs) of gold (Au), platinum nanoparticles (Pt) and boron (B) doped diamond electrode modified with nanoparticles of platinum, have been tested. Although modified electrodes have shown interesting ability toward arsenic detection, they also display many problems related to the immobilization of the mediator, its toxicity and cost. Considering these limitations, developing a cheap and easily constructed modified electrode with outstanding arsenic detection performance is an urgent and important research effort.

Ferrous oxide (Fe_3O_4) NPs is a low-cost, environmentally friendly and easy-prepared material, which has received much attention for arsenic removal because of their excellent adsorption ability (Gao et al., 2013; Wei et al., 2016). However, a conduction pathways for electrons below NPs can amplify current signal further enhancing sensitivity (Kumar et al., 2016). Nanocarbons based electrochemical sensors have improved performance due to their catalytic properties coupled with better conductivity, high loading capability and stability. Among them, graphene oxide (GO) is considered an excellent nanoplatform to develop electrochemical sensors, due to the nature of the atoms on its surface (Kumar et al., 2016).

In this paper, we present a novel electrochemical sensor made of $\text{Fe}_3\text{O}_4/\text{rGO}$ deposited on a GCE for electroanalytical detection of arsenic via cyclic voltammetry (CV) and square wave anodic stripping voltammetry (SWASV) in phosphate buffer solutions. $\text{Fe}_3\text{O}_4/\text{rGO}$ shows a very good relation between current response and amount of arsenic in a wide range of pollutants concentration, due to the electrocatalytic ability of rGO and the high adsorption ability of Fe_3O_4 towards As(III). Our sensor is easy to use, inexpensive and has allowed fast and sensitive detection of arsenic in non-acidic media (pH=7).

2. Experimental Section

2.1 Preparation of GO nanosheets

In a typical experiment (Sarno et al., 2016a; Sarno et al., 2016b), pure graphite powder was treated with H_2SO_4 , then, KMnO_4 was added at a temperature below 10°C . After 1 h, the system was heated up to 40°C for 30 min; during oxidation and intercalation, the volume of graphite expands and led to increased system viscosity. Then, the mixture was diluted with 100 mL of distilled water and 20 mL of H_2O_2 were added to the mixture to reduce residual KMnO_4 . After centrifugation, the resulting dispersion was dried and solid graphite oxide (GrO) was obtained. Further exfoliation was obtained by sonication and, after a suitable centrifugation, the supernatant phase (GO) was collected.

2.2 Preparation of $\text{Fe}_3\text{O}_4/\text{rGO}$

$\text{Fe}_3\text{O}_4/\text{GO}$ nanocomposite was prepared by thermolysis of Iron(III) acetylacetonate [$\text{Fe}(\text{acac})_3$] in the presence of GO, 1,2-hexadecanediol, oleic acid, oleylamine and benzyl ether (Sarno et al., 2015). The mixture was magnetically stirred and heated to 200°C for 2 h under nitrogen flow. Then, under a blanket of nitrogen, it was heated to reflux ($\sim 300^\circ\text{C}$) for 1 h and cooled to room temperature. A black material was obtained after intense washing and centrifugation.

2.3 Materials characterization.

The characterization of materials was obtained by the combined use of different techniques. TEM images were obtained with a FEI Tecnai electron microscope operating at 200 kV with a LaB6 filament as the source of electrons. The preparation of samples for TEM analysis involved sonication in ethanol for 2–5 min and deposition on a carbon grid. XRD measurements were performed with a Bruker D8 X-ray diffractometer using $\text{CuK}\alpha$ radiation. Powder samples were outgassed in He flow at 523K for 12h before measurements. FT-IR spectra were acquired by a Vertex 70 Apparatus (Bruker Corporation). For the electrochemical measurements 4 mg of the samples were dispersed in 80 μl of 5 wt.% Nafion solution to form a homogeneous ink. Then, the ink was dip casted onto a glassy carbon electrode, 3 mm in diameter, to give a thin film. Cyclic voltammetry (CV) curves were obtained using a PGSTAT302N Autolab Instruments Metrohm, using saturated calomel as a reference electrode, graphite as counter electrode and loadable glassy carbon as working electrode. The measurements were performed in phosphate buffer solution (pbs) at pH 7, 0.1M and for the arsenic detection tests in a 1 mg/L solution of sodium (meta) arsenite (NaAsO_2 , Sigma-Aldrich, $\geq 90\%$).

3. Results and discussion

The morphological and internal structural of $\text{Fe}_3\text{O}_4/\text{rGO}$ nanocomposite were determined TEM analysis. The TEM images are showed in Figure 1, at increasing magnifications. They give a clear evidence that the as synthesized $\text{Fe}_3\text{O}_4/\text{rGO}$ nanocomposite consists of Fe_3O_4 NPs, mean diameter ~ 25 nm, dispersed on GO nanosheets. The TEM images reveal that the Fe_3O_4 nanoparticles are attached to the graphene sheets, even after the ultrasonication used to disperse the nanocomposites for TEM characterization.

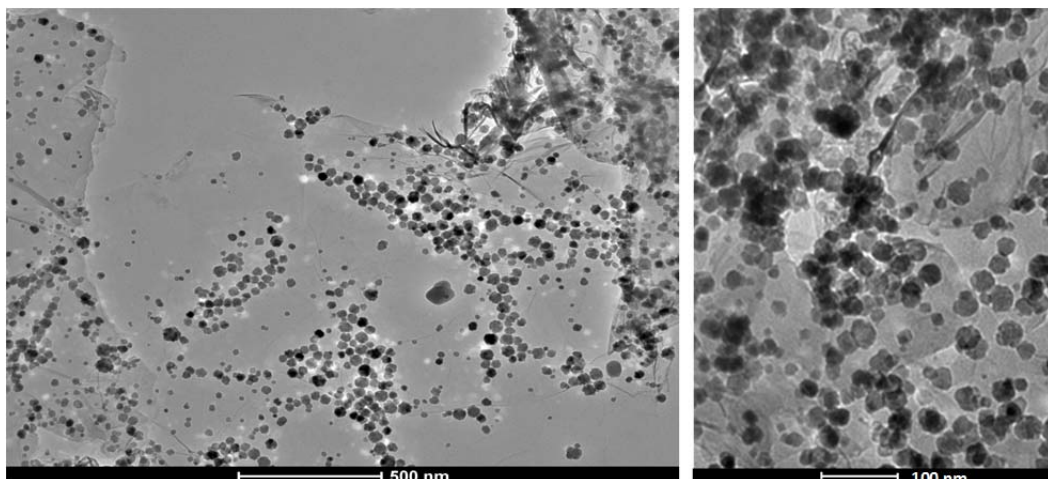


Figure 1: TEM images of as prepared of $\text{Fe}_3\text{O}_4/\text{rGO}$.

Figure 2 illustrates the detection strategy of As^{3+} based on the good adsorption ability of Fe_3O_4 NPs on the GO carpet. The As^{3+} is first adsorbed and reduced, after the redox to As^0 occurs producing a stripping arsenic peak (Davies et al., 2005).

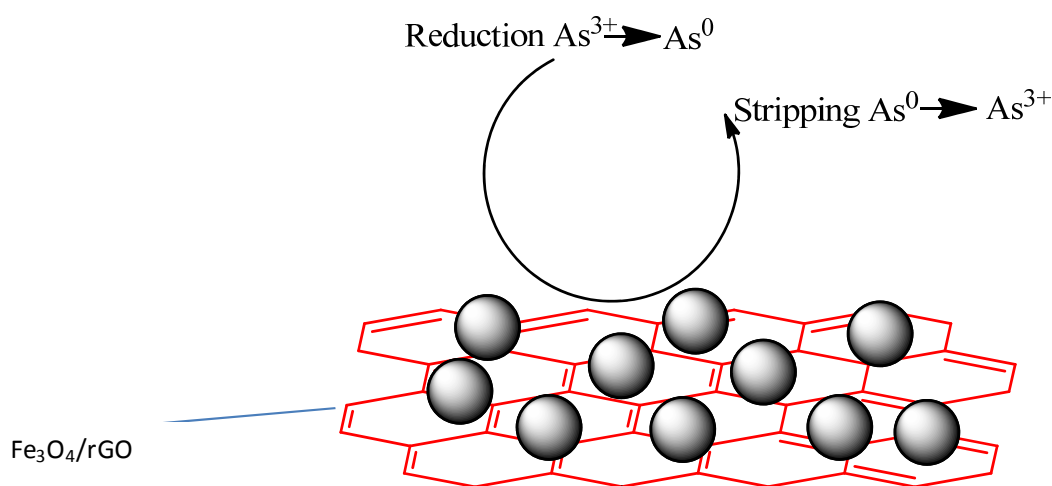


Figure 2: Scheme of detection strategy of As^{3+} based on adsorption ability of Fe_3O_4 NPs and electrocatalytic properties of rGO.

The diffraction peaks of GO was shown in Figure 3a. The peaks at around $2\theta = 10.4^\circ$ and 42.7° correspond to the (001) and (100) reflections of GO. The interlayer spacing calculated from the (001) reflection is 8.5 Å. The XRD pattern of GO indicates that the original graphite powders had almost been completely oxidized (Sarno et al., 2016b). The XRD profile of Fe_3O_4 NPs is shown in Figure 3b. The typical peak at $2\theta = 30.4^\circ$ (220), 35.4° (311), 43.2° (400), 53.7° (422), 57.4° (511) and 62.7° (440) of magnetite can be observed (Gao et al., 2011). In the XRD profile shown in Figure 3c for $\text{Fe}_3\text{O}_4/\text{rGO}$ the peaks of nanoparticles are clearly visible. On the other hand, the absence of the typical peaks of GO and the appearance of a weak peak at about 26° evidence the GO reduction. This occurred during the nanoparticles synthesis for both thermal and chemical phenomenon, leading to a reduced graphene oxide (rGO) with a good level of exfoliation (Yang et al., 2015). The infrared spectrum of GO (Figure 4) shows a complex pattern due to the presence of oxygen containing species formed by graphite oxidation (Eigler et al., 2012). The signals between 3600 and 3200 cm^{-1} are due to the O–H stretching vibration of free water, hydroxyl groups and adsorbed water molecules. Peak from carboxyl groups at about 1724 cm^{-1} is also present. The signal at 1615 cm^{-1} is related to the skeletal vibration of C=C bond, while the signal at 1403 cm^{-1} corresponds to O–H deformation vibrations from carboxylic groups (Stankovich et al., 2006). C–O vibrations of different species, mainly epoxy and hydroxyl groups, are present

in the range from 1300 to 800 cm^{-1} (Alhwaige et al., 2013). In particular, we assign the band at 1221 cm^{-1} to epoxy vibration group (Acik et al., 2010). The peak at 1059 cm^{-1} might also originate from skeletal C–C vibrational modes (Tamás Szabó et al., 2005). In the spectrum of Fe_3O_4 bands from the inorganic core and organic NPs coating can be observed (Sarno et al., 2016c). The $\text{Fe}_3\text{O}_4/\text{rGO}$ spectrum shows a lower number of peaks due unreduced oxygenated groups of the carbonaceous carpet. In particular, the peaks related to C=O bonds, epoxy groups and carboxyl groups disappeared, while the peak generated by skeletal vibration (1615 cm^{-1}) is still present.

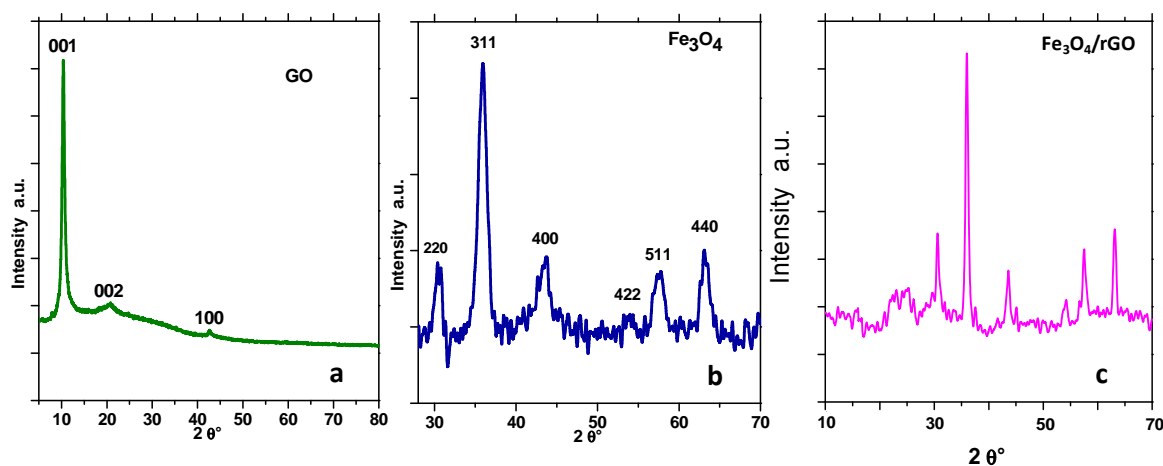


Figure 3: XRD spectrum of GO (a), Fe_3O_4 (b) and $\text{Fe}_3\text{O}_4/\text{rGO}$ (c).

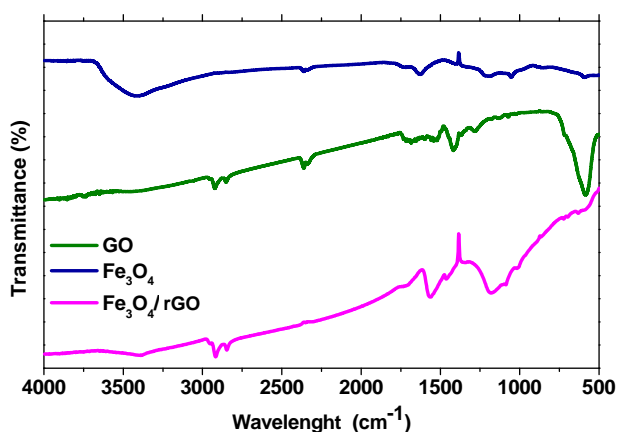


Figure 4: FT-IR spectra of GO, Fe_3O_4 and $\text{Fe}_3\text{O}_4/\text{rGO}$.

In order to verify the electrocatalytic activity of GO, Fe_3O_4 and $\text{Fe}_3\text{O}_4/\text{GO}$ on glassy carbon electrodes (GCE), electrochemical measurements in the presence of arsenite were carried out. In particular, the electrochemical behaviour of electrodes modified were further studied by cyclic voltammetry (CV) curves using 0,1M PBS at pH 7 in presence of arsenite. In particular, Figure 5a shows CV curves of the modified electrodes, for bare GCE (not shown here) no redox response to As^{3+} can be seen in the potential range from -1 V to 1 V. Fe_3O_4 NPs shows the anodic and cathodic peaks current which could be attributed to redox process of $\text{Fe}^{2+}/\text{Fe}^{3+}$ species. GO also shows a non-perfect rectangular shape during the scan between -1V until to 1 V. On the other hand, in the CV curve of $\text{Fe}_3\text{O}_4/\text{GO}$ two well defined peaks at about -0.18 V due to oxidation to As^{3+} , and in the reverse scan the peak around -0.44 V due to conversion of As^{3+} to As^0 (Kumar et al., 2016), can be seen. In Figure 5b some cyclic voltammograms of the $\text{Fe}_3\text{O}_4/\text{GO}$ in the presence of different concentrations of arsenite were shown. In particular, with increasing As^{3+} concentration the anodic peak currents increased and cathodic peaks disappeared. The catalytic peak currents are proportional to the concentration of arsenic in the wide range from 0.1 μM to 1 μM and from 10 μM to 150 μM . The linear correlation between the peaks current and the arsenic concentrations in solution are shown in Figure 5d and Figure 5e. To further examine the analytical performance of $\text{Fe}_3\text{O}_4/\text{rGO}$ on GCE towards arsenic, SWASV was employed because of its high

sensitivity in comparison to CV curves. Figure 5c presents the SWASV analytical characteristics for $\text{Fe}_3\text{O}_4/\text{rGO}$ at different concentrations of the analyte: deposition time 120 s, 12 mV step potential, 20 mV amplitude and 92 Hz frequency. The deposition step involved pre-concentration of As(III) species from the solution onto $\text{Fe}_3\text{O}_4/\text{rGO}$ electrode surface by reduction of As^{3+} to $\text{As}(0)$ at -0.35 V. On the other hand, a significant peak at -0.18 V is observed in the stripping scan from -0.5 to 0.8 V attributed to the oxidation of deposited $\text{As}(0)$ to As^{3+} species in stripping step. As(III) was detected with a sensitivity of $2.6 \mu\text{A ppb}^{-1}$ and a theoretical limit of detection (LOD) of 0.38 ppb.

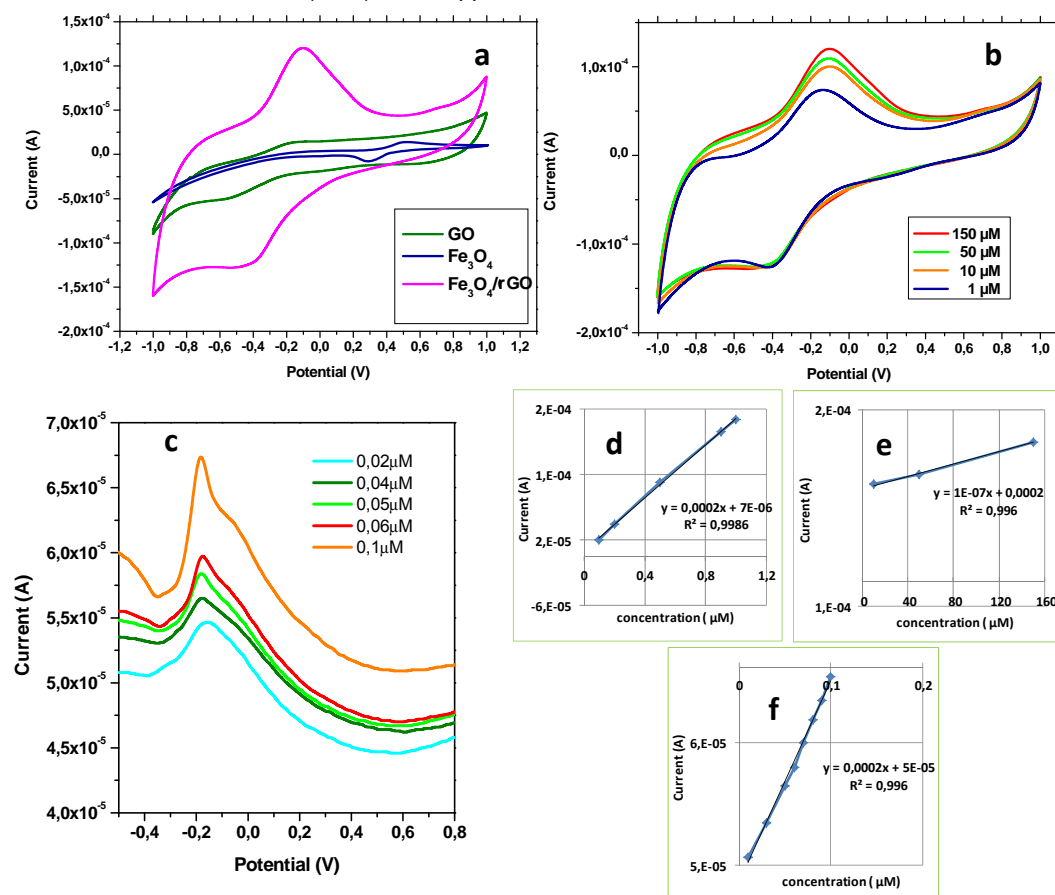


Figure 5: Comparison of cyclic voltammograms of GO, Fe_3O_4 and $\text{Fe}_3\text{O}_4/\text{rGO}$ on GCE in PBS at pH 7 in the potential range of $(-1-1)$ V at a scan rate of 2 mV/s in the presence of $50 \mu\text{M}$ of arsenite; (a). Cyclic voltammograms of $\text{Fe}_3\text{O}_4/\text{rGO}$ on GCE in pbs in pH 7 at a scan rate of 20 mV/s at increasing arsenic concentration: $1, 10, 50$ and $150 \mu\text{M}$; (b). SWASV with $\text{Fe}_3\text{O}_4/\text{rGO}$ on GCE in PBS at pH 7 at increasing arsenic concentration: $0.01, 0.05, 0.06, 0.07$ and $0.1 \mu\text{M}$; (c). Relation between arsenite concentration with peak current from cycling voltammetry as in (b); (d, e). Relation between arsenite concentration with peak current from SWASV as in (c); (f).

4. Conclusion

In this work, we have present a novel and stable electrochemical sensor made of $\text{Fe}_3\text{O}_4/\text{rGO}$ deposited on a glassy carbon electrode (GCE) for electroanalytical detection of As^{3+} , via cyclic voltammetry and square wave anodic stripping voltammetry in phosphate buffer solutions. The electrode made of Fe_3O_4 nanoparticles (25 nm mean diameter) on rGO shows a very good relation between current response and amount of analyte in a wide range of pollutant concentration, due to the electrocatalytic ability of rGO and the high adsorption ability of Fe_3O_4 towards As(III). Our sensor is easy to use, inexpensive and has allowed fast and sensitive detection of As (LOD= 0.38 ppb and sensitivity= $2.6 \mu\text{A ppb}^{-1}$) in a non-acidic media.

Reference

Acik M., Lee G., Mattevi C., Chhowalla M., Cho K., Chabal Y. J., 2010, Unusual infrared-absorption mechanism in thermally reduced graphene oxide, Nat. Mater. 9, 840.

- Alhwaige A., Agag T., Ishida H., Qutubuddin S., 2013, Biobased chitosan hybrid aerogels with superior adsorption: Role of graphene oxide in CO₂ capture, *RSC Adv.* 3, 16011.
- Alvarez-Llamas G.; de la Campa M. d. R.; Sanz-Medel A., 2005, *TrAC, Trends Anal. Chem.* 24, 28–36.
- Cai Y., 2000, Speciation and analysis of mercury, arsenic, and selenium by atomic fluorescence spectrometry, *TrAC Trends Anal. Chem.* 19, 62–66.
- Davies T.J., Compton R.G., 2005, The cyclic and linear sweep voltammetry of regular and random arrays of microdisc electrodes: Theory, *J. Electroanal. Chem.* 585, 63–82.
- Eigler S., Dotzer C., Hirsch A., 2012, Visualization of defect densities in reduced graphene oxide, *Carbon* 50, 3666–3673.
- Gao C., Yu X.Y., Xiong S.Q., Liu J.H., Huang X. J., 2013, Electrochemical Detection of Arsenic(III) Completely Free from Noble Metal: Fe₃O₄ Microspheres-Room Temperature Ionic Liquid Composite Showing Better Performance than Gold, *Anal. Chem.* 85, 2673–2680.
- Gao M., Li W., Dong J., Zhang Z., Yang B., 2011 Synthesis and characterization of superparamagnetic Fe₃O₄@SiO₂ core-shell composite nanoparticles, *World J. Condens. Matter Phys.*, 1, 49–54.
- Hignett G., Wadhawan J.D., Lawrence N.S., Hung, D.Q., Prado C., Marken F., Compton R. G., 2004, Electrochemical Detection of As(III) via Iodine Electrogenerated at Platinum, Gold, Diamond or Carbon-Based Electrodes, *Electroanalysis* 16, 897–903.
- Ivandini T.A., Sato R., Makide Y., Fujishima A., Einaga Y., 2006, Electrochemical Detection of Arsenic(III) Using Iridium-Implanted Boron-Doped Diamond Electrodes, *Anal. Chem.* 78, 6291–6298.
- Kumar S., Bhanjana G., Dilbaghi N., Kumar R., Umar A., 2016, Fabrication and characterization of highly sensitive and selective arsenic sensor based on ultra-thin graphene oxide nanosheets, *Sens. Actuators, B* 227, 29–34.
- Majid E., Harapovic S., Liu Y., Male K.B., Luong J.H.T., 2006, Electrochemical determination of arsenite using a gold nanoparticle modified glassy carbon electrode and flow analysis, *Anal. Chem.* 78, 762.
- Mandal B.K., Suzuki K.T., 2002, Arsenic round the world: a review, *Talanta* 58, 201.
- Sarno M., Cirillo C., Ponticorvo E., Ciambelli P., 2015, Synthesis and Characterization of FLG/Fe₃O₄ Nanohybrid Supercapacitor, *Chem. Eng. Trans.* 43, 727–732.
- Sarno M., Troisi A., Scudieri C., Ciambelli P., 2016a, Synthesis and Functionalization of Carbon Nanotubes and Graphene Based Supercapacitor for Arsenic Removal and Water Desalination: a Comparison, *Chem. Eng. Trans.* 47, 319–324.
- Sarno M., Baldino L., Scudieri C., Cardea S., Ciambelli P., Reverchon E., 2016b, Supercritical CO₂ processing to improve the electrochemical properties of graphene oxide, *J. Supercrit. Fluids* 118, 119–127.
- Sarno M., Cirillo C., Ponticorvo E., 2016c, High surface area monodispersed Fe₃O₄ nanoparticles alone and on physical exfoliated graphite for improved supercapacitors *J. Phys Chem. Solids* 99, 138–147.
- Stankovich S., Piner R. D., Nguyen S. T., Ruoff R. S., 2006, Synthesis and exfoliation of isocyanate-treated graphene oxide nanoplatelets, *Carbon* 44, 3342–3347.
- Story W.C., Caruso J.A., Heitkemper D.T., Perkins L., 1992, Elimination of the chloride interference on the determination of arsenic using hydride generation inductively coupled plasma mass spectrometry, *J. Chromatogr. Sci.* 30, 427.
- Sun Y.C., Mierzwa J., Yang M.H., 1997, New method of gold-film electrode preparation for anodic stripping voltammetric determination of arsenic (III and V) in seawater, *Talanta* 44, 1379.
- Tamás Szabó O. B., 2005, DRIFT study of deuterium-exchanged graphite oxide, *Carbon* 43, 3186–3189.
- Vandehoeck J., Waeles M., Riso R., Corre P., 2007, A stripping chronopotentiometric (SCP) method with a gold film electrode for determining inorganic arsenic species in seawater, *Anal. Bioanal. Chem.* 388, 929.
- Wei J., Li S.S., Guo Z., Chen X., Liu J.H., Huang X.J., 2016, Adsorbent Assisted in Situ Electrocatalysis: An Ultra-Sensitive Detection of As(III) in Water at Fe₃O₄ Nanosphere Densely Decorated with Au Nanoparticles, *Anal. Chem.* 88, 1154–1161.
- Welch C.M., Compton R.G., 2006, The use of nanoparticle in electroanalysis: review, *Anal. Bioanal. Chem.* 384, 601.
- World Health Organization, 2004. www.WHO.int/water_sanitation_health/water_quality/arsenic.html.
- Yang M., Yang Y., Liu Y., Shen G., Yu R., 2006, Platinum nanoparticles-doped sol-gel/carbon nanotubes composite electrochemical sensors and biosensors, *Biosens. Bioelectron.* 21, 1125.
- Yang X., Chen W., Huang J., Zhou Y., Zhu Y. & Li C. 2015, Rapid degradation of methylene blue in a novel heterogeneous Fe₃O₄@rGO@TiO₂-catalyzed photo-Fenton system. *Sci. Rep.* 5, 10632.
- Zhang N.; Fu N.; Fang Z.T.; Feng Y.H.; Ke L., 2011, Simultaneous multi-channel hydride generation atomic fluorescence spectrometry determination of arsenic, bismuth, tellurium and selenium in tea leaves, *Food Chem.* 124, 1185–1188.